Supporting Information

Ibiza *et al.* 10.1073/pnas.0711062105

SI Materials and Methods

Animals. Wild-type C57BL/6 and eNOS-null mice (C57BL/6, 129) were purchased from The Jackson Laboratory. All procedures involving animals and their care were approved by the Instituto de Salud Carlos III Bioethics and Animal Welfare Committee.

Antibodies, Cells, and Reagents. The anti-human CD3ε T3b mAb has been described in ref. 1. Other antibodies were sourced as follows: anti-mouse CD3 KT3 from Serotec; anti-eNOS mAb from BD PharMingen; anti-eNOS pAb (1185–1205) from Sigma–Aldrich; anti-phospho-eNOS (pSer^{1179}), -ERK1/2, and -phospho-ERK1/2 from Cell Signaling; anti-K-Ras (F234: sc-30) and -N-Ras (F155: sc-31) from Santa Cruz Biotechnology; anti-cH-Ras (Y132-ab32417) from Abcam; anti-pan-Ras (clone MC57) from Upstate; anti-nitrosocysteine from A.G. Scientific; anti-Golgin-97 from Molecular Probes; goat anti-mouse (GAM) H&L chain-specific IgG from Calbiochem. TRITC-conjugated swine anti-rabbit (SAR), rabbit anti-mouse (RAM), and FITC-conjugated goat anti-mouse (GAM) IgG were from DAKO.

The human lymphoid T cell line CH7C17 was grown in RPMI medium 1640 (Invitrogen) supplemented with 10% FBS and antibiotics (400 μg/ml hygromycin and 4 μg/ml puromycin). The Raji and HOM-2 lymphoblastoid B cell lines were each grown in RPMI medium 1640 supplemented with 10% FBS. Highly purified mouse T lymphoblasts were obtained as described in ref. 1.

Staphylococcus enterotoxin-B (SEB) was from Toxin Technology. The fluorescent cell tracker chloromethyl derivative aminocoumarin (CMAC), and Bodipy TR C_5-ceramide were from Molecular Probes. Poly-L-lysine, *N*-nitro-L-arginine (L-NAME), and propidium iodide were from Sigma–Aldrich. DETA-NO and DEA-NONOate were from Alexis Biochemicals. Streptavidin–horseradish peroxidase was from Amersham Biosciences. Cy5-labeled annexin V was from BD PharMingen. *N*-[6-(biotinamido)hexyl]-3′-(2′-pyridyldithio) propionamide (biotin-HPDP) and neutravidin–agarose were from Pierce.

Plasmids, DNA Constructs, and Fusion Proteins. Plasmids encoding HA-tagged wild-type and C118S mutant Ras proteins and enhanced cyan fluorescent protein (ECFP) fusions of wild-type and C1118S Ras mutant (pECFP-KZ-AU5-H-Ras, and -N-Ras) were obtained as described in ref. 2. pECFP-AU5-K-Ras4B-wt and pECFP-HA-K-Ras4B-C118S were prepared by amplifying from the corresponding pCEFL constructs by PCR (forward primer, 5′-AGTTTCCCCACACTGAGTGGGTG-GAGACTGAAGTT-3′; reverse, 5′-ATTGTCGACTTA-CATAATTACACACTTT-3′). PCR products were digested with BglII and SalI and cloned into the BglII–SalI sites of pECFP-C1. The plasmid encoding enhanced yellow fluorescent protein (EYFP) fusion of the Ras-binding domain (RBD) of Raf-1 (pEYFP-Raf-RBD-Raf-1) was obtained by digestion and subcloning into the BglII–EcoRI sites of pEYFP-C1. pcDNA3-eNOS-GFP was generously provided by W. Sessa (Yale University, New Haven, CT). The G2A eNOS point mutant (G2A-GFP) was generated with the QuikChange site-directed mutagenesis kit (Stratagene) and verified by DNA sequencing. The GST-RBD-Raf-1 fusion protein (containing the Ras-binding domain of Raf-1 fused to GST) was purified from *Escherichia coli* B121 (DE3) as described in ref. 3.

Quantitative RT-PCR. Quantitative RT-PCR analysis of eNOS mRNA expression in T lymphoblasts from wild-type C57BL/6 and eNOS-null mice was performed as described in ref. 1.

NO Production. Release of NO from cells was monitored for 30 min with an ISO-NOP NO electrode (World Precision Instruments) as described in ref. 1.

Confocal Fluorescence Microscopy. Raji antigen-presenting cells (APCs) (4×10^5) were loaded with CMAC, incubated for 30 min with or without 0.5 μg/ml SEB, and then mixed with equal numbers of eNOS- or G2A-GFP CH7C17 cells that were transiently transfected with ECFP fusions of wild-type N-, K-, or H-Ras or their corresponding C118S mutants. When indicated, cells were cotransfected with pEYFP-RBD-Raf-1. Cells were plated on poly-L-lysine-coated coverslips and allowed to settle for 10 min at 37°C in humidified incubation chambers. Cells were fixed for 10 min in 2% paraformaldehyde in PBS at room temperature and rinsed in TBS. For immunofluorescence of phosphorylated eNOS, cells were permeabilized for 30 s in 0.2% Triton X-100 and incubated with anti-eNOS-pSer^{1179} pAb, with TRITC-conjugated SAR as secondary. For double immunofluorescence staining of eNOS and Golgin-97, cells were fixed and permeabilized as described above and then incubated with rabbit anti-eNOS (1185–1205) pAb (with TRITC-conjugated SAR IgG as secondary) followed by extensive washing in TBS and incubation with mouse anti-Golgin-97 mAb [FITC-conjugated $F(ab')_2$ GAM IgG as secondary]. In this case, the digital assignments of color staining for eNOS and Golgin-97 were green and red, respectively. Mounted coverslips were viewed under a Leica TCS-SP confocal laser scanning unit attached to a Leica DM1RB inverted microscope equipped with a HCX PL APO CS 63× NA 1.32 oil-immersion objective lens (Leica).

To assess automatically the spatial distribution of EYFP-RBD-Raf-1, ECFP-K-Ras, -N-Ras, and -N-Ras(C118S) on the Golgi and plasma membrane of eNOS- and G2A-GFP cells, images were acquired with settings that in each case allowed the maximum signal detection below the saturation limits of the detectors. Excitation wavelengths for fluorochromes were 351 and 364 nm for CMAC, 458 nm for pECFP, 488 nm for GFP, and 514 nm for pEYFP-RBD-Raf-1. Images were captured sequentially to avoid signal cross-contamination. Photomultiplicator sensitivity and laser intensity were always below 700 mV and 70%, respectively. The emission apertures for fluorescence detection were 370–450 nm for CMAC, 465–485 nm for pECFP, 500–514 nm for GFP, and 550–596 nm for pEYFP-RBD-Raf-1. Six to eight confocal Z sections were necessary to capture the entire fluorescent signal. The ratio of fluorescence intensity between the cellular regions of interest was calculated in a single Z plane, corresponding with the maximum fluorescence plane, by using Leica Confocal Software, version 2.61 (Leica Microsystems). At least 100 cells were analyzed for each sample. For fluorescence profile analysis, cross-sections (8 μm) were drawn through a field including the Golgi apparatus or a field far from the Golgi to compare the intensity and distribution of fluorescence. The quantification graphs obtained use the color codes corresponding to cell staining.

Detection of *S*-Nitrosylation. *S*-nitrosylated proteins were detected by the biotin switch method (4, 5) with the recently described reduction step modification (6). Cells were stimulated in the dark with anti-CD3 as described above. Cell lysates were mixed with 4 volumes of blocking buffer (225 mM Hepes, 0.9 mM EDTA, 0.09 mM neocuproine, 2.5% SDS, and 20 mM MMTS) at 50°C for 20 min with agitation. Proteins were precipitated with acetone and resuspended with HENS buffer (250 mM Hepes, 1

mM EDTA, 0.1 mM neocuproine, 1% SDS) containing 50 mM ascorbate to reduce nonmodified nitrosothiols. One-third volumes of 4 mM biotin-HPDP in DMF were added, and the samples were incubated for 90 min at room temperature in the dark. Proteins were then precipitated with acetone and precipitates resuspended in HENS and 3 volumes of neutralization buffer (20 mM Hepes, 100 mM NaCl, 1 mM EDTA, 0.5% Triton X-100). At this point, biotinylation was detected by immunoblotting. For purification of biotinylated proteins, samples were incubated with neutravidin–agarose beads for 60 min at room temperature with agitation. Beads were washed four times with wash buffer (25 mM Hepes, 600 mM NaCl, 1 mM EDTA, 0.5% Triton X-100) and once with elution buffer without 2-mercaptoethanol (20 mM Hepes, 100 mM NaCl, 1 mM EDTA). Proteins were eluted with elution buffer containing 100 mM 2-mercaptoethanol for 20 min at 37°C with gentle agitation. Supernatants were collected, separated by 15% SDS/PAGE, and immunoblotted for Ras detection.

Densitometric Analysis. Quantitative estimation of activated proteins was performed by densitometric analysis of immunoblots with Image Gauge v.346 software (Fujifilm). Densitometric results corresponding to at least three independent experiments were normalized to total protein loadings, and values represent the fold induction ratios (means ± SEM) with respect to time = 0 (value,1).

Flow Cytometry Analysis of Apoptosis. Flow cytometry analysis of cell death was performed as described in ref. 7. Briefly, T cells (3×10^5) were stimulated with CD3 T3B Ab (5 μg/ml) plus goat anti-mouse IgG cross-linking for 24 h at 37°C and then washed in HBSS and resuspended in 500 μl of binding buffer containing 250 ng/ml Cy5-labeled annexin V and 250 ng/ml propidium iodide. The mixture was incubated in the dark for 15 min at room temperature, and the cell binding of annexin V and propidium iodide was analyzed by flow cytometry (FACscan; Becton Dickinson). CFP-positive cells were gated for analysis of annexin V expression on wild-type and C118S N-Ras-transfected eNOS-GFP cells.

Statistical Analyses. Data within groups were compared by using one-way ANOVA with Newman–Keul's post hoc correction for multiple comparisons; statistical significance was set at P values of 0.05 or lower.

1. Ibiza S, *et al.* (2006) Endothelial nitric oxide synthase regulates T cell receptor signaling at the immunological synapse. *Immunity* 24:753–765.
2. Renedo M, *et al.* (2007) Modification and activation of Ras proteins by electrophilic prostanoids with different structure are site-selective. *Biochemistry* 46:6607–6616.
3. Jorge R, *et al.* (2002) HSos1 contains a new amino-terminal regulatory motif with specific binding affinity for its pleckstrin homology domain. *J Biol Chem* 277:44171–44179.
4. Jaffrey SR, Erdjument-Bromage H, Ferris CD, Tempst P, Snyder SH (2001) Protein *S*-nitrosylation: A physiological signal for neuronal nitric oxide. *Nat Cell Biol* 3:193–197.
5. Martinez-Ruiz A, *et al.* (2005) *S*-Nitrosylation of Hsp90 promotes the inhibition of its ATPase and endothelial nitric oxide synthase regulatory activities. *Proc Natl Acad Sci USA* 102:8525–8530.
6. Forrester MT, Foster MW, Stamler JS (2007) Assessment and application of the biotin switch technique for examining protein *S*-nitrosylation under conditions of pharmacologically induced oxidative stress. *J Biol Chem* 282:13977–13983.
7. van Genderen H, *et al.* (2006) *In vitro* measurement of cell death with the annexin A5 affinity assay. *Nat Protoc* 1:363–367.

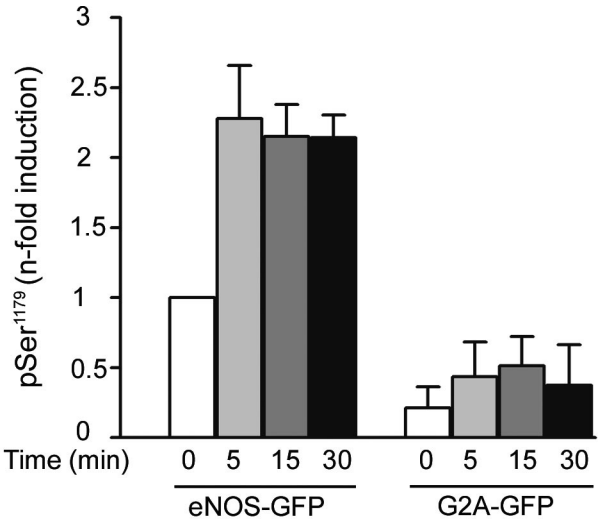

Fig. S1. Quantitative analysis corresponding to Fig. 1*C*. eNOS- and G2A-GFP phosphorylation at Ser^{1179} ($pSer^{1179}$) in T cells exposed to APCs. The chart shows normalized Western blot band densities for $pSer^{1179}$, presented as fold induction with respect to eNOS-GFP phosphorylation at time 0. Data are the means ± SEM of three independent experiments.

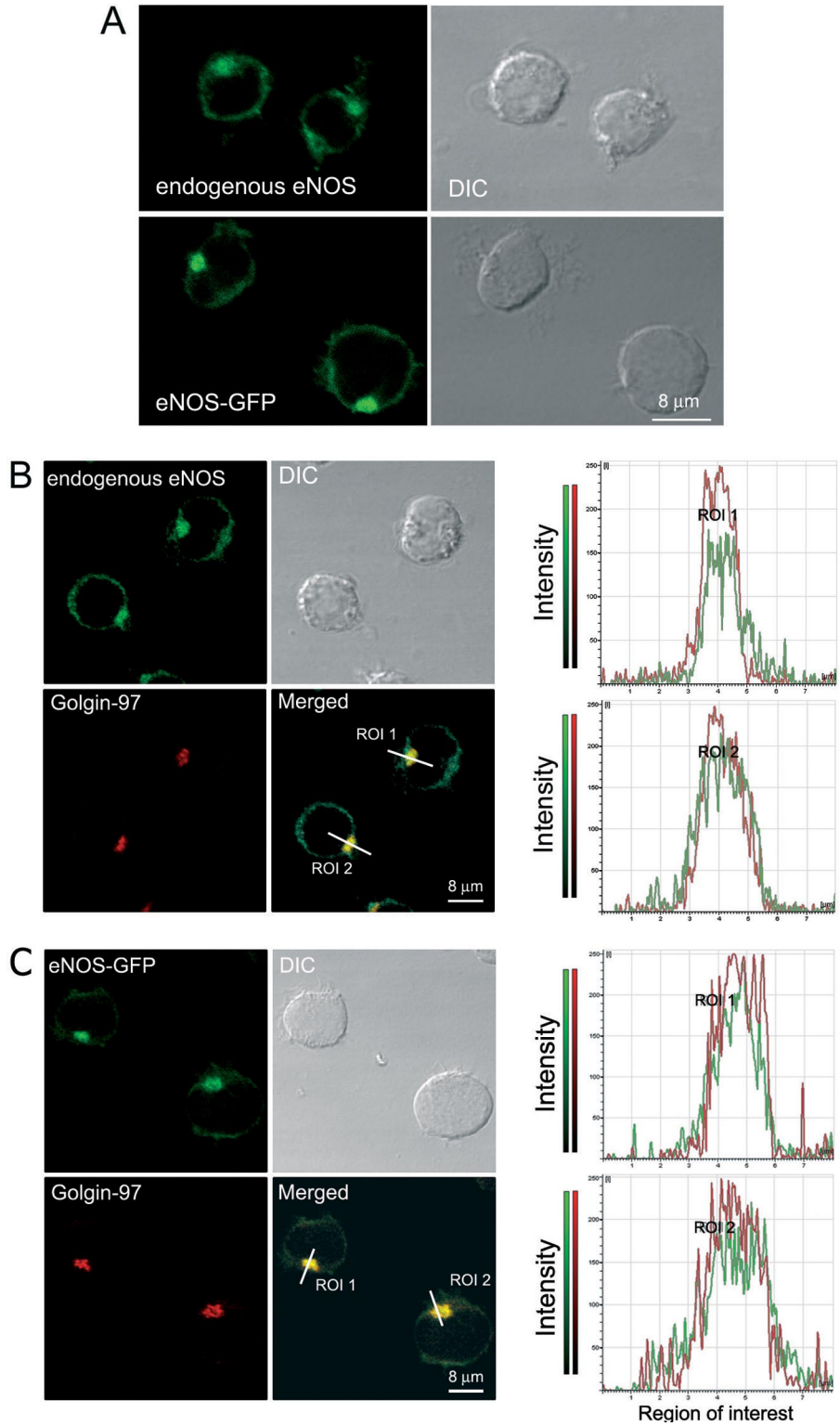

Fig. S2. eNOS subcellular localization in T cells. Paraformaldehyde-fixed nontransfected or eNOS-GFP-expressing CH7C17 T cells were permeabilized with 0.2% Triton X-100 and stained with the corresponding Abs as described in *SI Material and Methods*. (*A*) Staining pattern of endogenous eNOS and transfected eNOS-GFP in CH7C17 cells. (*B*) Localization analysis of endogenous eNOS and Golgin-97 in CH7C17 cells (double immunofluorescence staining). (*C*) Localization analysis of eNOS-GFP and Golgin-97 in eNOS-GFP cells. Fluorescence intensity profiles to the right of *B* and *C* show codistribution of Golgin-97 with endogenous eNOS (*B*) and with eNOS-GFP (*C*) along 8-μm sections through the regions of interest (ROI) indicated in the merged image. DIC images are also shown.

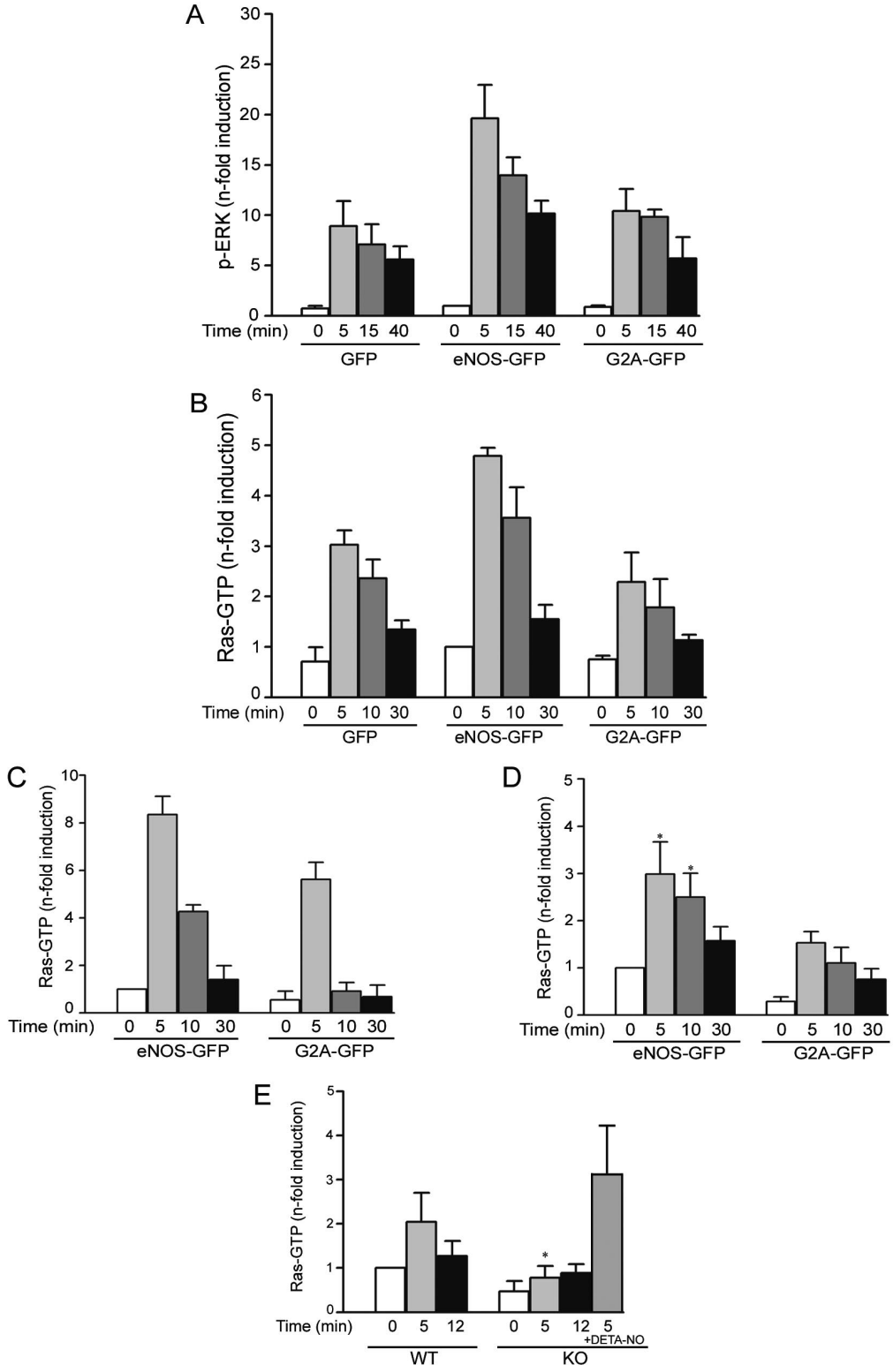

Fig. S3. Quantitative analysis corresponding to Fig. 2. Charts show normalized Western blot band densities presented as fold inductions with respect to the eNOS-GFP condition (*A–D*) or wild-type mouse T lymphoblasts (*E*) at time 0. (*A*) ERK activation (phosphorylation) corresponding to Fig. 2*A*. (*B–D*) Ras activation (GTP-bound Ras) corresponding to Fig. 2 *B–D*. (*E*) Ras activation in wild-type (WT) versus eNOS$^{-/-}$ (KO) T lymphoblasts, corresponding to Fig. 2*F*. Data are the means ± SEM of three independent experiments. *, $P \leq 0.05$ compared with time-paired values for G2A-GFP (*D*) or WT (*E*).

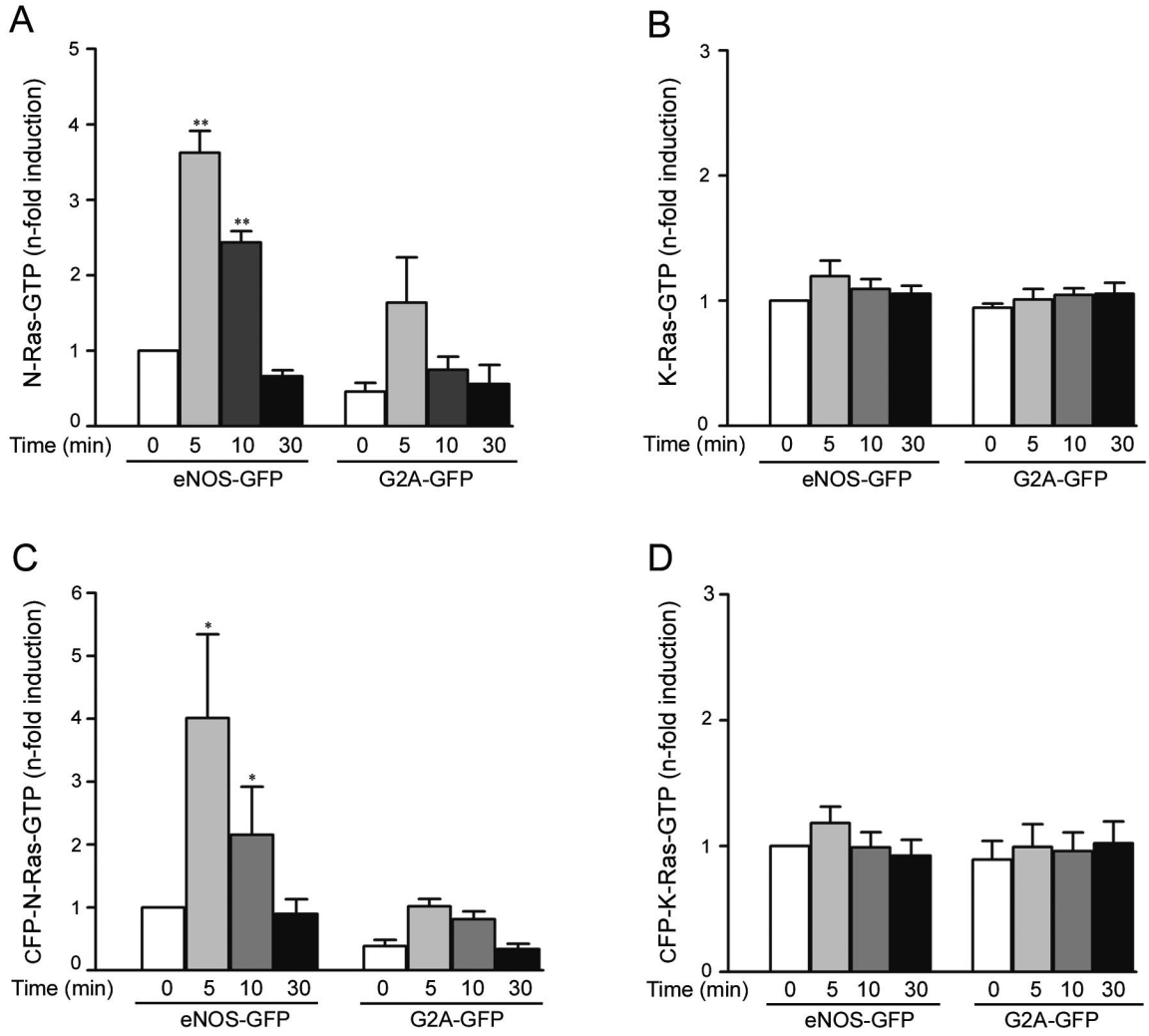

Fig. S4. Quantitative analysis corresponding to Fig. 3: N- and K-Ras. (*A* and *B*) Activation (GTP binding) of endogenous N-Ras (*A*) and K-Ras (*B*), corresponding to Fig. 3*A*. (*C* and *D*) Activation of transfected CFP-N-Ras (*C*) and CFP-K-Ras (*D*), corresponding to Fig. 3*B*. Data are the means ± SEM of three independent experiments. **, $P \leq 0.01$ and *$P \leq 0.05$ compared with time-paired values for G2A-GFP.

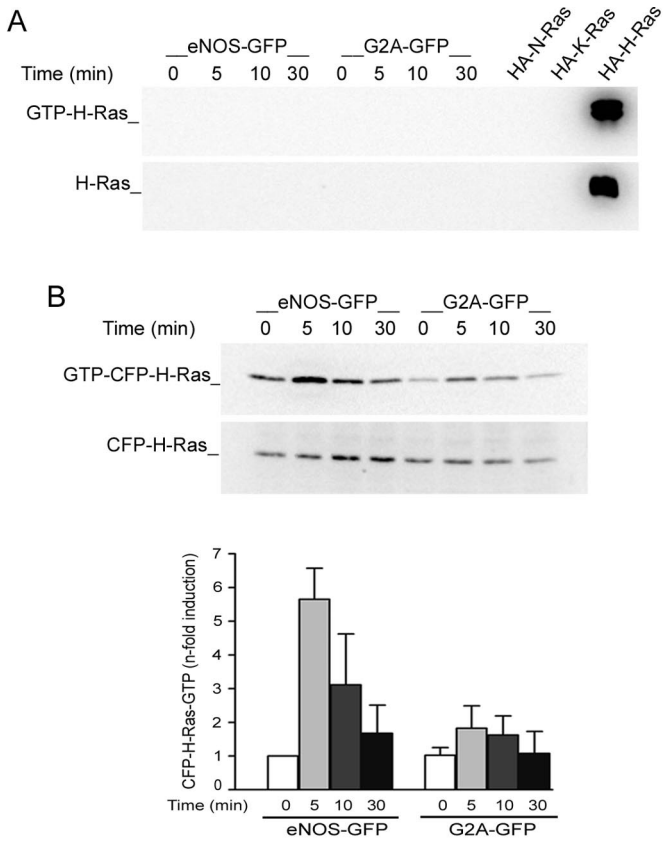

Fig. S5. H-Ras expression and activation in eNOS-GFP cells. (*A*) Time course activation of endogenous H-Ras. eNOS- and G2A-GFP cells were stimulated with CD3 Ab with IgG cross-linking for the times indicated. As controls of antibody specificity, lanes were loaded with extracts of cells expressing similar amounts of HA-tagged N-, K-, and H-Ras. (*B*) eNOS- and G2A-GFP cells transiently expressing CFP-H-Ras were stimulated with SEB-pulsed Raji APCs for the times indicated. The expression of activated and total H-Ras was analyzed by immunoblotting with an anti-H-Ras mAb. Blots are representative of three independent experiments. The chart in *B* shows corresponding quantification of activated H-Ras (means ± SEM).

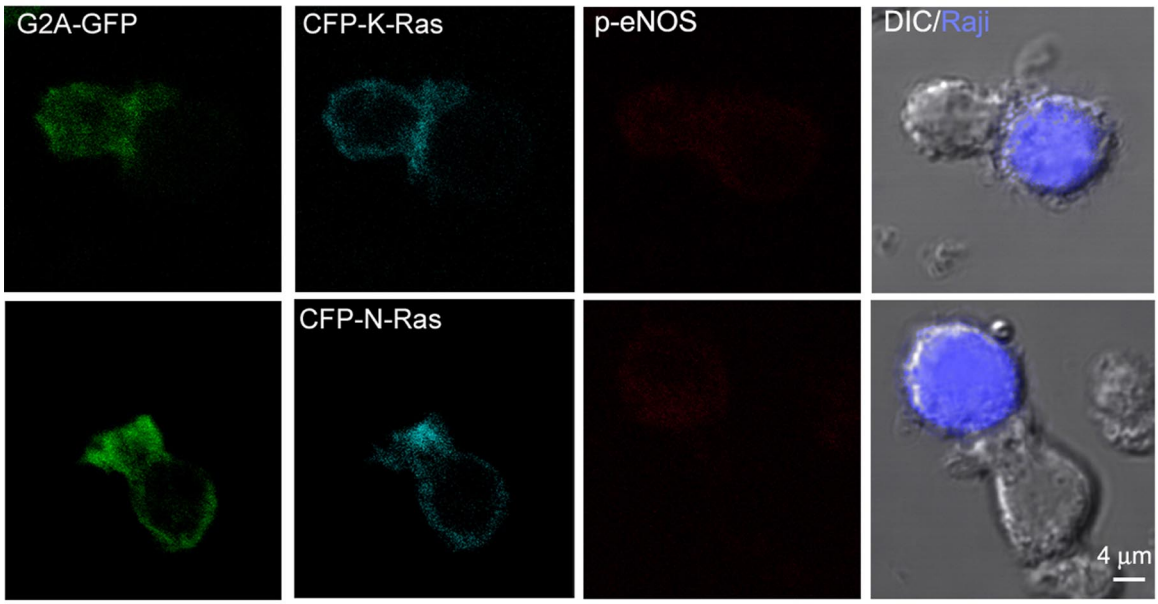

Fig. S6. eNOS phosphorylation in G2A-GFP T cells forming conjugates with APCs. G2A-GFP cells transiently expressing CFP-K-Ras or -N-Ras were mixed with SEB-pulsed Raji APCs for 10 min. Cells were fixed and then stained with eNOS-pSer^{1179} pAb. The subcellular localization of phospho-eNOS (red), eNOS (green), and Ras (cyan) was analyzed by confocal fluorescence microscopy. CMAC staining of Raji APCs (blue) is superposed on DIC images.

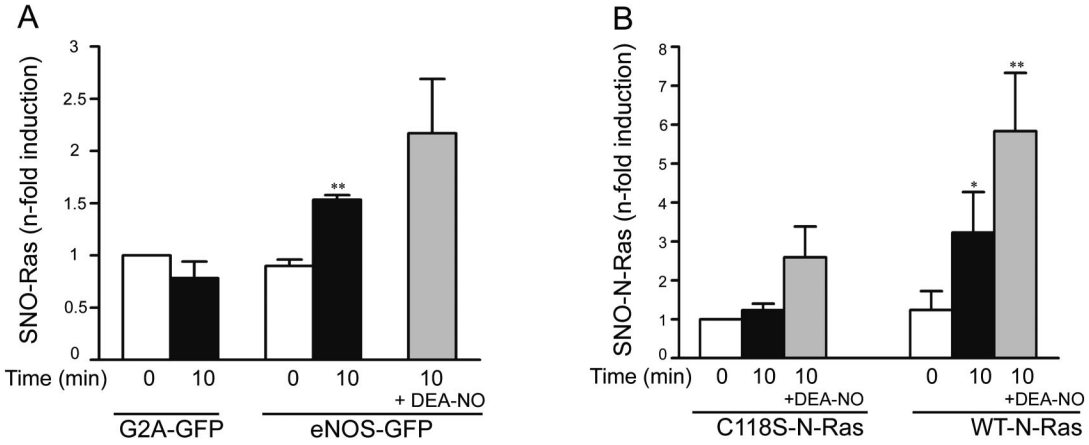

Fig. S7. Quantitative analysis corresponding to Fig. 6 *A* and *B*: *S*-nitrosylation of endogenous and transfected N-Ras. (*A*) *S*-nitrosylation of endogenous Ras corresponding to Fig. 6*A*, shown as fold inductions with respect to the G2A-GFP condition at time 0. (*B*) *S*-nitrosylation of transfected N-Ras corresponding to Fig. 6*B*, shown as fold inductions with respect to cells expressing C118S-N-Ras at time 0. Data are the means ± SEM of three independent experiments. **, $P \leq 0.01$ and * $P \leq 0.05$ compared with time-paired values for G2A-GFP (*A*) or C118S-N-Ras (*B*).

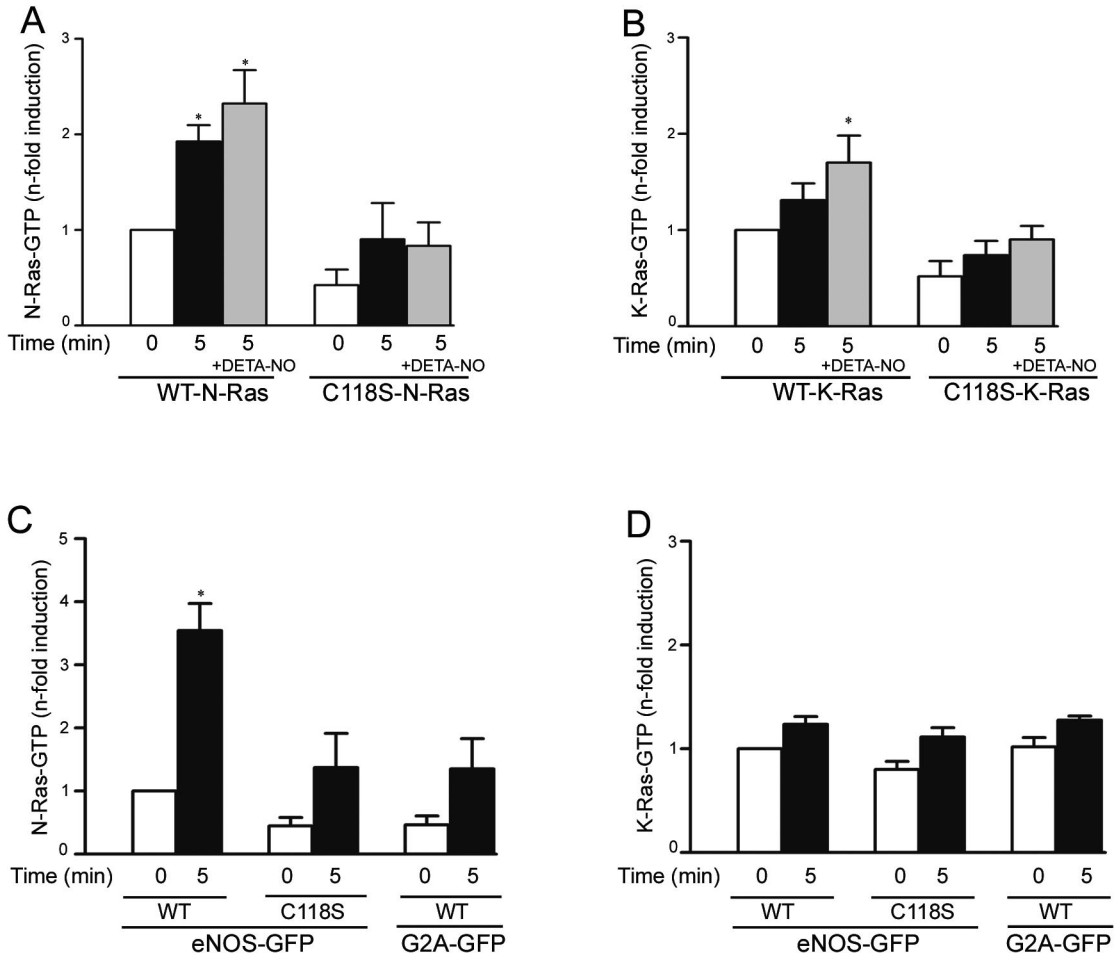

Fig. S8. Quantitative analysis corresponding to Fig. 6 *C* and *D*: GTP-bound N-, and K-Ras. (*A* and *B*) Activation (GTP binding) of CFP-N-Ras (*A*) and -K-Ras (*B*) corresponding to Fig. 6*C*. (*C* and *D*) Activation of CFP-N-Ras (*C*) and CFP-K-Ras (*D*) corresponding to Fig. 6*D*. Data are the means ± SEM of at least three independent experiments. *, $P \leq 0.05$ compared with time-paired values for C118S-Ras (*A*–*C*) and G2A-GFP (*C*).

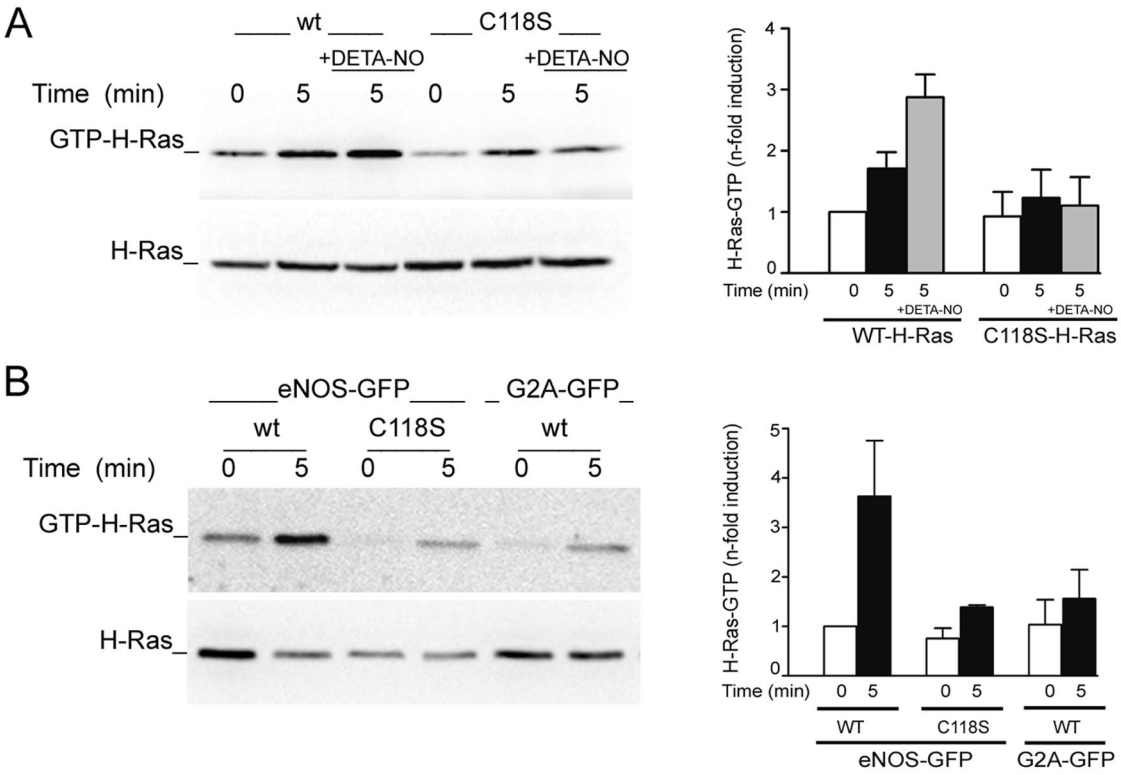

Fig. S9. Comparison of the activation of wild-type and C118S H-Ras in response to NO. (*A*) Activation of wild-type and C118S H-Ras by NO donors. CH7C17 cells were transiently transfected with CFP fusions of wild-type (WT) or C118S H-Ras. Thirty-six hours after transfection, cells were stimulated with CD3 Ab plus IgG cross-linking for the times indicated in the presence or absence of 100 μM DETA-NO. Cell extracts were pulled down with GST-RBD-Raf-1, and H-Ras activation was detected by immunoblotting. (*B*) Activation of wild-type and C118S H-Ras by eNOS-derived NO. G2A-GFP cells expressing wild-type CFP-H-Ras and eNOS-GFP cells expressing wild-type or C118S H-Ras were stimulated with CD3 Ab, and H-Ras activation was determined as in *A*. Charts show corresponding normalized fold inductions with respect to activation of wild-type CFP-H-Ras in CH7C17 cells (*A*) and eNOS-GFP cells (*B*) at time 0. Data are the means ± SEM of three independent experiments.

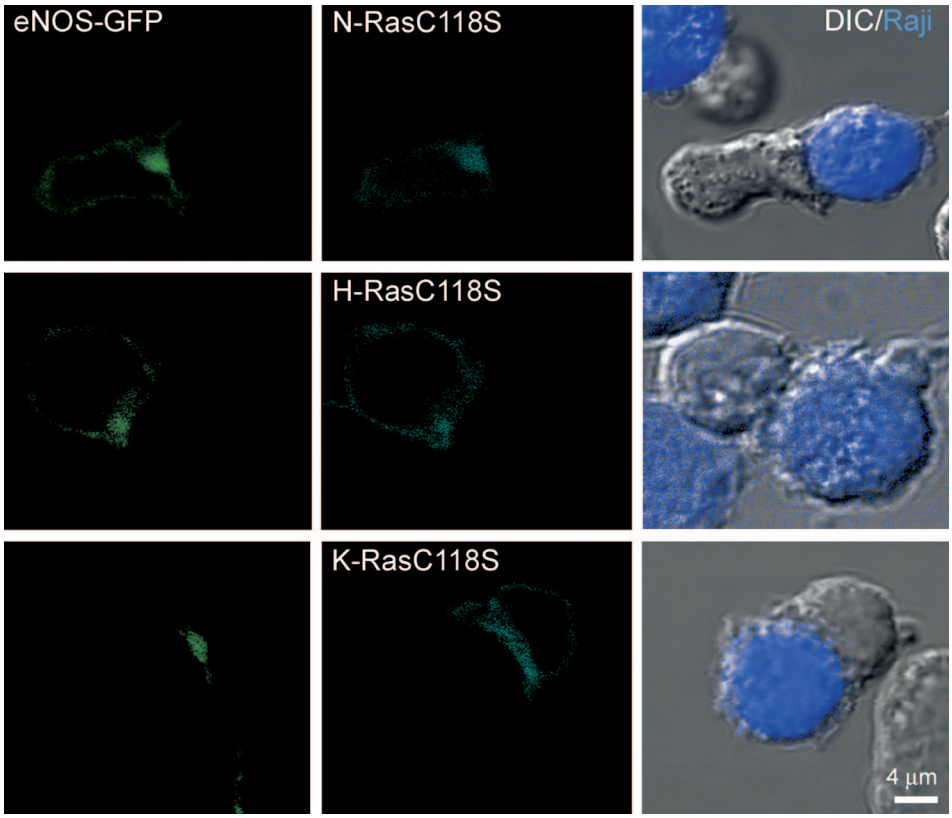

Fig. S10. Localization of C118S Ras in antigen-specific T cell–APC conjugates. eNOS-GFP cells transiently expressing C118S CFP-N-Ras, -H-Ras, or -K-Ras were mixed with SEB-pulsed Raji APCs for 10 min, and the subcellular localization of eNOS (green) and Ras (cyan) was analyzed by confocal fluorescence microscopy. CMAC staining of Raji APCs (blue) is superposed on DIC images.

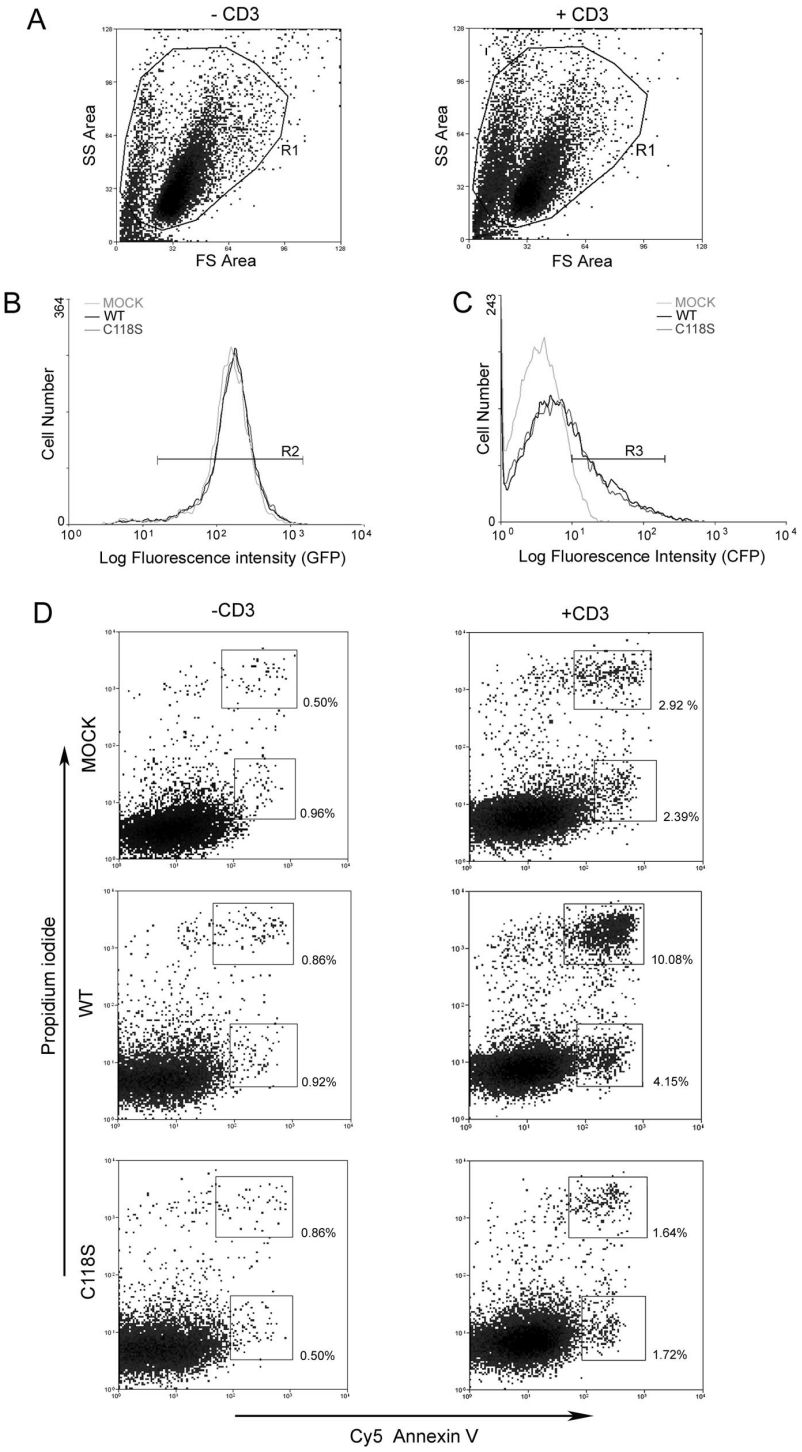

Fig. S11. Cys^{118} is important for N-Ras-dependent activation-induced death in eNOS-GFP T cells. eNOS-GFP cells transfected with wild-type CFP-N-Ras (WT), C118S CFP-N-Ras (C118S), or empty vector (MOCK) were incubated for 24 h without (−CD3) or with CD3 Ab (+CD3) (5 μg/ml) plus goat anti-mouse IgG cross-linking (10 μg/ml). Cells were harvested and stained with Cy5-labeled annexin V and propidium iodide as described in *SI Material and Methods*. For flow cytometric determination of activation-induced cell death, cells were simultaneously gated for the side- and forward-scatter regions corresponding to the fluorescence signals of nonstimulated (−CD3) or CD3-stimulated (+CD3) cells (*A*, R1), GFP (*B*, R2), and CFP (*C*, R3). (*D*) Dot plots of annexin V and propidium iodide staining in nonstimulated (−CD3) or CD3-stimulated (+CD3) cells in the intersection of these gated regions (R1∩R2∩R3). (*Inset, Bottom Right*) Cells in the early phase of apoptosis (*Inset, Top Right*) Cells in the late phase of apoptosis. For each condition, 13,000 events are represented. The corresponding percentages of early and late cell death are indicated. Data shown are representative of three independent experiments.